Letter

Spin- and flux-gap renormalization in the random Kitaev spin ladder

Wen-Han Kao [*] and Natalia B. Perkins [†]
School of Physics and Astronomy, University of Minnesota, Minneapolis, Minnesota 55455, USA

(Received 13 May 2022; accepted 24 August 2022; published 9 September 2022)

We study the Kitaev spin ladder with random couplings by using the real-space strong-disorder renormalization group (SDRG) technique. This model is the minimum model in Kitaev systems that has conserved plaquette fluxes, and its quasi-one-dimensional geometry makes it possible to study the strong-disorder fixed points for both spin- and flux-excitation gaps. In the Ising limit where the x-type Ising couplings compete with the z-type couplings and the y-type couplings are small but nonzero, the behavior of the spin gap is consistent with a random transverse-field Ising chain, but the flux gap is dominated by the y-type couplings. In the XX limit, while the x- and y-type couplings are locally equal and renormalized simultaneously, the z-type couplings are not renormalized drastically and lead to nonuniversal disorder criticality at low-energy scales. We show that different types of fractionalized degrees of freedom in the disordered Kitaev model can result in different critical behaviors, as long as its fluxes can survive the perturbative treatment.

DOI: 10.1103/PhysRevB.106.L100402

Introduction. Quantum spin liquid (QSL), an exotic magnetic phase with fractionalized spin excitations and intricate entanglement structure, has been pursued both theoretically and experimentally since its first proposal by Anderson in 1973 [1]. Theoretical models and candidate materials with strong geometrical or exchange frustration are expected to greatly reduce the ordering temperature and reveal the quantum fluctuations. However, the presence of residual interactions in real systems usually leads to magnetic ordering and shatters the hope of finding QSL. Nevertheless, various compounds were discovered with no magnetic ordering, even down to the lowest measurable temperature, and commonly the quenched randomness was found to serve as a potential cause of the sustaining disordered phase and intriguing dynamics of low-energy degrees of freedom [2–6]. Therefore the competition between quantum fluctuations and randomness raises a critical question about the true nature of the low-energy phase in those materials. For example, the peculiar low-energy excitations found in the second generation of Kitaev materials [7–9] may be ascribable to spin fractionalization in weakly disordered QSL [10–12], but it may also relate to the random-singlet (RS) phase in strongly disordered magnets [13]. The RS phase was first proposed in the studies of the random spin chains by a real-space perturbation scheme called the strong-disorder renormalization group (SDRG) [14–16]. This method has been shown to be asymptotically exact if the random distribution broadens infinitely through the iteration, and the ground-state wave function of the RS is a product state of singlets with a variety of distances. In this regard, the RS phase is not a QSL, despite having quantum critical features.

Even though the strong-disorder phenomenology for Kitaev systems has been discussed in different scenarios [13,17], the direct application of SDRG is still lacking and the fate of flux degrees of freedom under disorder remains an open question. Previous studies of SDRG on two-dimensional models have shown that the connectivity on each site grows drastically in the iteration [18–21], and thus it is presumed that any properties derived from elementary plaquettes of the lattice, such as geometrical frustration and plaquette fluxes, will be destroyed by the local perturbation schemes such as SDRG.

In this Letter we study a quasi-one-dimensional Kitaev spin ladder with plaquette fluxes. There exists a dual transformation of this model [22], which transforms it into a chain Hamiltonian with (dual) spins and fluxes preserved by the local perturbative treatment. Thus the random Kitaev spin ladder provides a fruitful playground to study the SDRG flow of both the (dual) spin- and flux-excitation energies and the corresponding disorder criticalities. Our numerical SDRG results show that the spin- and flux-gap energy scale can either be a universal function following the SDRG fixed-point distribution, or a nonuniversal one affected by the initial random distributions. Here we present our main findings and defer full technical details of the extended SDRG methodology to a forthcoming publication [23].

Strong-disorder renormalization group. The main idea of SDRG is to successively decimate out the larger-energy (shorter-time) degrees of freedom in real space and scrutinize the flow of random distributions throughout the iteration. The low-energy physics, phase transitions, and corresponding critical exponents can be extracted from the fixed-point solutions. Moreover, for simple one-dimensional models such as random Heisenberg chain and random transverse-field Ising chain (RTIC), the analytical solution of the RG flow equation can be obtained even in the off-critical Griffiths region away from infinite-disorder fixed point (IDFP) [24]. In more complicated models, numerical SDRG was applied extensively in order to extract the low-energy physics governed by strong-disorder fluctuations. Comprehensive reviews of SDRG can be found in Refs. [21,25].

[*] kao00018@umn.edu
[†] nperkins@umn.edu

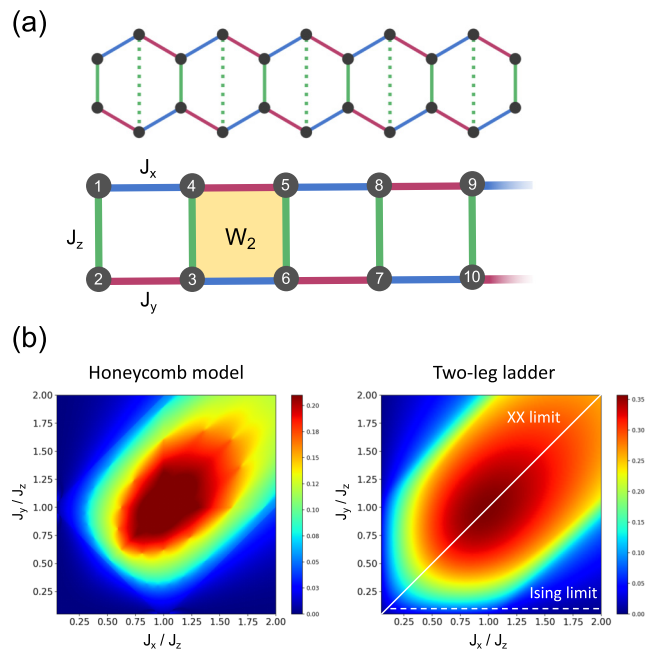

FIG. 1. (a) Kitaev spin ladder derived from one row of the honeycomb lattice. The shaded plaquette denotes the conserved flux operator $W_2 = -\sigma_3^y \sigma_4^x \sigma_5^x \sigma_6^y$. (b) The lowest flux-excitation gap for the pure Kitaev honeycomb model and two-leg ladder. The white solid (dashed) line denotes the XX limit (Ising limit) of the model considered in this work. In the Ising limit, the small but nonzero J_y is required in order to have finite flux gaps.

Model. We consider a spin-1/2 two-leg Kitaev spin ladder with alternating x and y Ising couplings on the legs and z couplings on the rungs as in Fig. 1(a). The sites are labeled as a one-dimensional chain with third-neighbor x couplings:

$$\mathcal{H} = -\sum_{l=1}^{N/2} \left[J_x \sigma_{2l-1}^x \sigma_{2l+2}^x + J_y \sigma_{2l}^y \sigma_{2l+1}^y + J_z \sigma_{2l-1}^z \sigma_{2l}^z \right]. \quad (1)$$

This can be seen as a minimum model reduced from the Kitaev honeycomb model [26] that still has conserved flux operators $W_l = -\sigma_{2l-1}^y \sigma_{2l}^x \sigma_{2l+1}^x \sigma_{2l+2}^y$ on each plaquette. We apply the duality transformation [22]

$$\sigma_j^z = \prod_{k=j}^{N} \tau_k^z, \quad \sigma_j^y = \tau_{j-1}^y \tau_j^y, \quad (2)$$

such that the effective Hamiltonian (excluding the boundary terms) becomes a transverse-field XY dual-spin chain:

$$\mathcal{H} = -\sum_{j}^{L} \left[J_x W_j \tau_j^x \tau_{j+1}^x + J_y \tau_j^y \tau_{j+1}^y + J_z \tau_j^z \right]. \quad (3)$$

Note that we relabel the indices since the couplings and fields are present only on odd sites $(2l-1)$ such that the length of the chain is $L = N/2$. In addition, the operators of even sites $(2l)$ form a set of local conserved quantities $W_l = \tau_{2l-2}^y \tau_{2l}^z \tau_{2l+2}^y$ with eigenvalues ± 1. In fact, this is precisely the plaquette flux operator of the original spin model. In this dual Hamiltonian, the fluxes are present explicitly so that we can separate flux sectors by different sets of W eigenvalues. According to Lieb's theorem [27], the ground-state sector of the pure Kitaev ladder is in the π-flux phase where all $W = -1$. With open boundary conditions, the flux can be singly excited from -1 to $+1$. The lowest flux excitation energy is plotted in Fig. 1(b), and it resembles the flux-gap phase diagram of the Kitaev honeycomb model [28].

Note that in Eq. (3), the original spin operators σ_i are transformed into the dual-spin operators τ_i and flux operators W_i. This is similar to the Majorana representation of the Kitaev honeycomb model, where spin can fractionalize into the Majorana fermions and flux gauge fields. Therefore we can define two types of the lowest excitation energy in our model: the *spin gap* refers to the first dual-spin excitation of a given flux sector, and the *flux gap* refers to the ground-state energy difference between an arbitrary flux sector and the π-flux sector. We note that the *spin gap* in the dual model is not the same as a spin gap in the original model of Eq. (1). In the random model, all the couplings and fields are quenched disordered and given by arbitrary random distributions $R(J_x)$, $Q(J_y)$, and $P(J_z)$.

XX limit. In this limit, the x and y couplings on the same bond are equal $J_{x,j} = J_{y,j} \equiv J_j$ and thus only two independent distributions $R(J)$ and $P(J_z)$ are considered. In the bond-decimation scheme [Fig. 2(a), lower panel], we derive the RG rule from the four-site example with the largest energy scale $\Omega = J_2$ and treat the rest of the terms as perturbation. The two spins in the middle are then frozen in their local ground state with a large decimation gap 2Ω, similar to the formation of a random singlet in the random Heisenberg chain. Spins on site 1 and 4 then form a renormalized coupling with a new flux variable:

$$\tilde{J} = \frac{J_1 J_3}{\Omega}, \quad \tilde{W} = W_1 W_2 W_3. \quad (4)$$

With $W_2 = \pm 1$, $J_{z,2}$ and $J_{z,3}$ will contribute to the different constant energy shifts in the perturbation theory [29], and this gives rise to the flux gap

$$\Delta E_f(W_2) = \frac{J_{z,2} J_{z,3}}{\Omega}. \quad (5)$$

In the site decimation scheme, we consider a three-site example with $\Omega = J_{z,2}$ [Fig. 2(b)]. The strongest field tends to align the spin on site 2, and renormalized couplings are formed between site 1 and site 3 as $\tilde{J} = J_1 J_2 / \Omega$ with $\tilde{W} = W_1 W_2$. However, in site decimation the neighboring transverse fields are also modified and become flux dependent:

$$\tilde{J}_{z,1} = J_{z,1} - \frac{J_1^2}{\Omega} W_1, \quad \tilde{J}_{z,3} = J_{z,3} - \frac{J_2^2}{\Omega} W_2. \quad (6)$$

In later decimation steps, if $\tilde{J}_{z,1}$ or $\tilde{J}_{z,3}$ happen to be the new Ω of the system, this flux-dependent term will become the flux gap for W_1 or W_2. One important observation from the decimation rules is that the couplings are renormalized much faster than the fields, such that the site decimation becomes dominant in the low-energy limit [23]. Numerically, we implemented SDRG in a similar way to the studies of random Heisenberg chain and RTIC for the spins and additionally calculate the local flux gaps from Eqs. (5) and (6) for each decimation step, if applicable (see details in Ref. [29]).

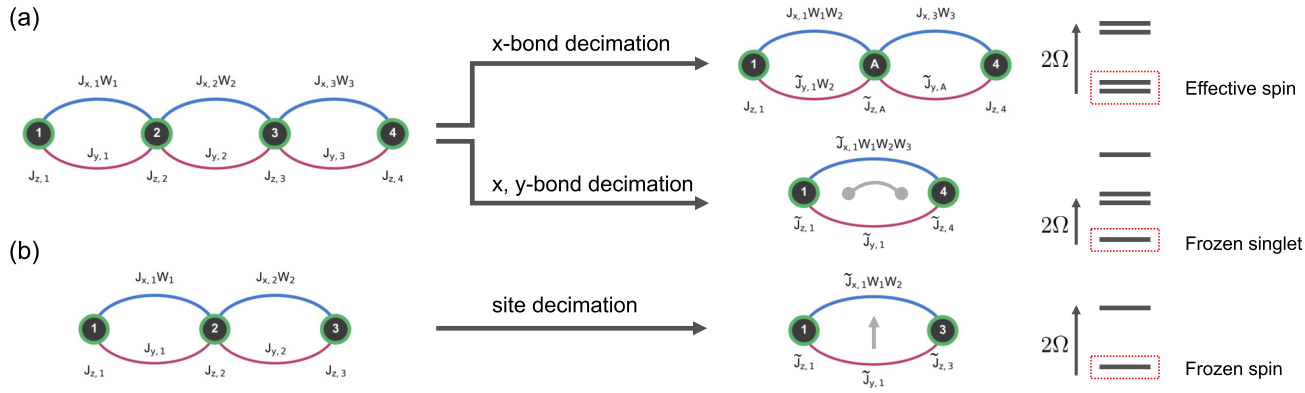

FIG. 2. Decimation rules for the Kitaev spin ladder in the Ising and XX limits. (a) Ising limit (upper panel): The x-bond decimation with the largest energy scale $\Omega = J_{x,2}$. The upper doublet formed by site 2 and site 3 is integrated out, and the lower doublet forms an effective spin-1/2 site A with renormalized couplings and an on-site effective field. XX limit (lower panel): x and y couplings on the same bond are equal, $J_{x,j} = J_{y,j} \equiv J_j$, so that they are simultaneously decimated with the largest energy scale $\Omega = J_2$. Spins on sites 2 and 3 form a local ground state with a large decimation gap 2Ω, and spins on sites 1 and 4 are coupled by a renormalized interaction with a new flux variable. (b) The site decimation with the largest energy scale $\Omega = J_{z,2}$. Site 2 is aligned by the transverse field, and the neighboring sites are coupled by the renormalized couplings.

Ising limit. In this limit we consider the scale of J_y to be much smaller than J_x and J_z, such that x-bond and site decimations are dominant in SDRG. Therefore the fixed-point solution of RTIC can be applied for J_x and J_z. Even though J_y is considered to be very small, it is required to be finite in order to have nonzero flux excitation energies. In the bond-decimation scheme ($\Omega = J_{x,2}$), the strongest Ising coupling leads to a low-energy doublet which is kept as a renormalized spin, as shown in the upper panel of Fig. 2(a). The low-energy effective Hamiltonian can be rigorously derived via the Schrieffer-Wolff transformation [30–32], and the effective transverse field on this renormalized spin is (see details of the derivation in Ref. [29])

$$\tilde{J}_{z,A} = J_{y,2} W_2 - \frac{J_{z,2} J_{z,3}}{\Omega}. \tag{7}$$

The site decimation rule is derived from the three-site example and is similar to that in the XX limit.

Since the decimation rules in the Ising limit are more complicated than in the XX limit, we executed the SDRG calculations on the π-flux sector and all the one-flux excitation sectors for each random realization. The flux gaps are then computed from the energy difference between different sectors, instead of being estimated from the decimation rules. The validity of the method is verified by comparing the small-sized results in exact diagonalization [23].

In the numerical SDRG calculation, we consider different phases according to the initial uniform distributions of the couplings with different widths:

$$J_x \in [0, \Delta_x], \quad J_y \in [0, \Delta_y], \quad J_z \in [0, \Delta_z]. \tag{8}$$

For the critical phase we set $g = \Delta_z/\Delta_x = 1$, and for the off-critical (Griffiths) phase we take $g = 1/4$ or 4. In all cases we set Δ_y to be much smaller such that y-bond decimation happens rarely. In Fig. 3 we show the distributions of spin and flux gaps from all the one-flux excitation sectors. Note

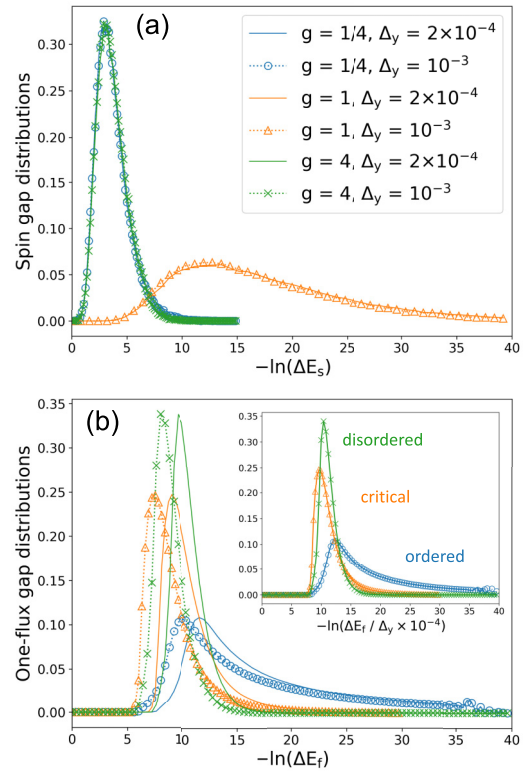

FIG. 3. Distribution of (dual) spin and fluxes gaps of different phases for various small Δ_y in the Ising limit. (a) The spin-gap distribution for π-flux sector and one-flux excitation sectors. The distributions of the first excitation gap are shown for the disordered ($g = 4$) and critical phase ($g = 1$), and the second gap is chosen for the ordered phase ($g = 1/4$). (b) Distribution of the one-flux excitation gaps. The inset shows that the Δ_y dependence can be removed by dividing Δ_y for each gap. All data are obtained from the numerical SDRG with 10^5 random samples of the $L = 128$ chain.

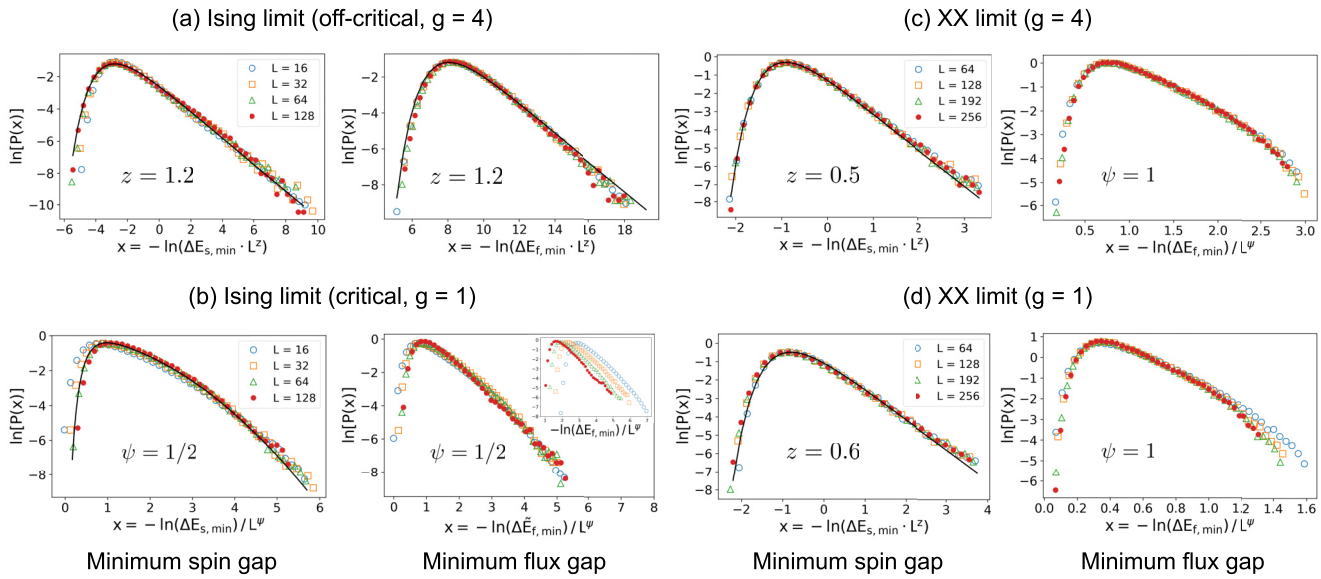

FIG. 4. Extreme-value statistics on the (dual) spin and flux gaps. The black solid lines in (a), (c), and (d) represent the fitting of the Fréchet distribution [Eq. (9)]. For the fitting curve of IDFP with $\psi = 1/2$ in (b), the approximate form in Ref. [33] is used. All data are obtained from the numerical SDRG of $10^5 - 10^6$ random samples with various system sizes.

that in the disordered ($g = 4$) and critical ($g = 1$) phases we collect the first spin gap, while in the ordered ($g = 1/4$) phase we use the second spin gap, due to the fact that the first spin gap corresponds to the finite-size effect of degenerate ground states in the ordered phase [29,34,35]. For the spin gaps, the ordered and disordered phases have identical distribution because of the duality with respect to the critical point. Also, as shown in Fig. 3(a), the spin-gap distributions are almost unchanged by tuning the width Δ_y. However, in the flux-gap distributions shown in Fig. 3(b), a clear shift is observed for different Δ_y in all three phases. This suggests that while the spin gaps are functions of J_x and J_z and almost independent of J_y values, the flux gaps in general have a linear dependence on J_y.

Extreme-value statistics. We first consider the Ising-limit result. Based on the analytical solution of RTIC [36,37], in the disordered phase the extreme-value statistics of the minimum spin gap follow the Fréchet distribution with $u = u_0 \Delta E_s L^z$:

$$P(\ln u) = \frac{1}{z} u^{1/z} \exp(-u^{1/z}), \tag{9}$$

where the dynamical exponent z is determined [24,38] by the equation $z \ln(1 - z^{-2}) = -\ln g$, and with $g = 4$ we obtain $z \approx 1.211$. In Fig. 4(a), the finite-size scaling of our numerical SDRG result shows that both spin and flux gaps follow the analytical form, indicating the fixed-point behavior.

At the critical point of RTIC, the minimum-gap distribution has a rather complicated form [37] but the finite-size scaling can be done by noting that $-\ln \Delta E \sim L^{1/2}$ from the infinite-disorder fixed-point solution. Our results show that the minimum-spin-gap distributions perfectly match this scaling law [Fig. 4(b), left panel], but the minimum-flux-gap distributions of different sizes cannot collapse in the same way [Fig. 4(b), inset of the right panel]. This suggests the nonuniversal behavior for the flux gaps at the critical point, which can be understood as follows.

In the critical case ($g = 1$), bond decimation is equally important as the site decimation. However, the former may lead to a flux gap with $J_{y,i}$ from Eq. (7). Thus the local flux gap for W_2 can have the general expression

$$\Delta E_f(W_2) = 2J_{y,2} + \text{renormalized terms} \ldots, \tag{10}$$

such that the leading term is determined by the initial distribution of J_y. This explains why in Fig. 3 it has linear dependence of Δ_y, but in Fig. 4(b) a nonuniversal size scaling is observed. To verify this, we show that the nonuniversal behavior in extreme-value statistics on flux gaps can be removed by defining $\Delta \tilde{E}_f(W_i) \equiv \Delta E_f(W_i)/J_{y,i}$. The resulting curves [Fig. 4(b), right panel] are indeed scaled as the infinite-disorder fixed-point solution.

In the XX limit, with the dominant site decimation at low energies at and away from $g = 1$, the extreme-value statistics of the spin gaps simply gives the Fréchet distribution for uniform distributions, as shown on the left panel of Figs. 4(c) and 4(d) [39]. On the other hand, the flux-gap distributions show a trend of broadening similar to the IDFP but with a different exponent $\psi = 1$. Even in the case of power-law initial distributions, this scaling behavior remains robust [23]. The above results demonstrate again that different strong-disorder criticalities can happen for the flux excitations.

Conclusion. In the pursuit of the quantum spin liquid phase in real materials, it was argued that disorder-induced random-singlet phase is responsible for the observed power-law divergence in magnetic specific heat and susceptibility [13]. In this work we applied the SDRG scheme to the random Kitaev spin ladder model and showed that strong-disorder criticality appears not only for the spins but also for the local conserved quantities. Even though other types of interaction may present in real systems, the validity of our approach relies on that Kitaev coupling remains the largest energy scale in each step of SDRG iteration. We showed that the flux degrees

of freedom in this model can be preserved by the duality transformation and thus survive the local perturbation theory of SDRG. We also showed that the fluxes may reveal different criticalities compared to the (dual) spin degrees of freedom. Moreover, we found that the power-law exponent of the flux-gap distribution depends on the type of initial distribution of couplings. This points out a new complexity in understanding the strong-disorder effect in frustrated spin systems and is worth further theoretical inquiries. Finally, we remark that the importance of the Griffiths-like effect is pointed out in a recent paper for understanding the nonuniversal power-law exponents of Majorana excitations in the disordered Kitaev model with static fluxes [40]. Our work is a complementary study, since the extended SDRG can also reveal the disorder criticality of fluxes. Since the flux-gap energy scale is usually far below the (dual) spin gaps, we anticipate that the transition between different power laws can potentially be seen in the low-temperature specific heat of the disordered Kitaev candidate materials [7].

Acknowledgments. We thank Yu-Ping Lin, Eduardo Miranda, and Chi-Yun Lin for fruitful discussions. W.-H.K. and N.B.P. acknowledge support from NSF DMR-1929311 and the support of the Minnesota Supercomputing Institute (MSI) at the University of Minnesota.

[1] P. W. Anderson, Mater. Res. Bull. **8**, 153 (1973).
[2] D. E. Freedman, T. H. Han, A. Prodi, P. Müller, Q.-Z. Huang, Y.-S. Chen, S. M. Webb, Y. S. Lee, T. M. McQueen, and D. G. Nocera, J. Am. Chem. Soc. **132**, 16185 (2010).
[3] K. Riedl, R. Valentí, and S. M. Winter, Nat. Commun. **10**, 2561 (2019).
[4] H. Yamaguchi, M. Okada, Y. Kono, S. Kittaka, T. Sakakibara, T. Okabe, Y. Iwasaki, and Y. Hosokoshi, Sci. Rep. **7**, 16144 (2017).
[5] H. Murayama, Y. Sato, T. Taniguchi, R. Kurihara, X. Z. Xing, W. Huang, S. Kasahara, Y. Kasahara, I. Kimchi, M. Yoshida, Y. Iwasa, Y. Mizukami, T. Shibauchi, M. Konczykowski, and Y. Matsuda, Phys. Rev. Research **2**, 013099 (2020).
[6] S.-H. Do, C.H. Lee, T. Kihara, Y.S. Choi, S. Yoon, K. Kim, H. Cheong, W.-T. Chen, F. Chou, H. Nojiri, and K.-Y. Choi, Phys. Rev. Lett. **124**, 047204 (2020).
[7] K. Kitagawa, T. Takayama, Y. Matsumoto, A. Kato, R. Takano, Y. Kishimoto, S. Bette, R. Dinnebier, G. Jackeli, and H. Takagi, Nature (London) **554**, 341 (2018).
[8] S. Trebst and C. Hickey, Phys. Rep. **950**, 1 (2022).
[9] F. Bahrami, M. Abramchuk, O. Lebedev, and F. Tafti, Molecules **27**, 871 (2022).
[10] J. Knolle, R. Moessner, and N. B. Perkins, Phys. Rev. Lett. **122**, 047202 (2019).
[11] W.-H. Kao, J. Knolle, G. B. Halász, R. Moessner, and N. B. Perkins, Phys. Rev. X **11**, 011034 (2021).
[12] W.-H. Kao and N. B. Perkins, Ann. Phys. **435**, 168506 (2021).
[13] I. Kimchi, J. P. Sheckelton, T. M. McQueen, and P. A. Lee, Nat. Commun. **9**, 4367 (2018).
[14] S.-K. Ma, C. Dasgupta, and C.-K. Hu, Phys. Rev. Lett. **43**, 1434 (1979).
[15] C. Dasgupta and S.-K. Ma, Phys. Rev. B **22**, 1305 (1980).
[16] D. S. Fisher, Phys. Rev. B **50**, 3799 (1994).
[17] S. Sanyal, K. Damle, J. T. Chalker, and R. Moessner, Phys. Rev. Lett. **127**, 127201 (2021).
[18] O. Motrunich, S.-C. Mau, D. A. Huse, and D. S. Fisher, Phys. Rev. B **61**, 1160 (2000).
[19] Y.-C. Lin, R. Mélin, H. Rieger, and F. Iglói, Phys. Rev. B **68**, 024424 (2003).
[20] I. A. Kovács and F. Iglói, Phys. Rev. B **82**, 054437 (2010).
[21] I. A. Kovács and F. Iglói, J. Phys.: Condens. Matter **23**, 404204 (2011).
[22] X.-Y. Feng, G.-M. Zhang, and T. Xiang, Phys. Rev. Lett. **98**, 087204 (2007).
[23] W.-H. Kao and N. B. Perkins (unpublished).
[24] F. Iglói, Phys. Rev. B **65**, 064416 (2002).
[25] F. Iglói and C. Monthus, Eur. Phys. J. B **91**, 290 (2018).
[26] A. Kitaev, Ann. Phys. **321**, 2 (2006).
[27] E. H. Lieb, Phys. Rev. Lett. **73**, 2158 (1994).
[28] Y. Motome and J. Nasu, J. Phys. Soc. Jpn. **89**, 012002 (2020).
[29] See Supplemental Material at http://link.aps.org/supplemental/10.1103/PhysRevB.106.L100402 for the derivations of SDRG decimation rules and the technical details of numerical SDRG.
[30] J. R. Schrieffer and P. A. Wolff, Phys. Rev. **149**, 491 (1966).
[31] R. Vosk and E. Altman, Phys. Rev. Lett. **112**, 217204 (2014).
[32] D. Pekker, G. Refael, E. Altman, E. Demler, and V. Oganesyan, Phys. Rev. X **4**, 011052 (2014).
[33] Y.-P. Lin, Y.-J. Kao, P. Chen, and Y.-C. Lin, Phys. Rev. B **96**, 064427 (2017).
[34] F. Iglói and C. Monthus, Phys. Rep. **412**, 277 (2005).
[35] R. Juhász, Y.-C. Lin, and F. Iglói, Phys. Rev. B **73**, 224206 (2006).
[36] D. S. Fisher, Phys. Rev. Lett. **69**, 534 (1992).
[37] D. S. Fisher and A. P. Young, Phys. Rev. B **58**, 9131 (1998).
[38] I. A. Kovács, T. Pető, and F. Iglói, Phys. Rev. Research **3**, 033140 (2021).
[39] Even though the dynamical exponent is only slightly dependent on g in the case of uniform distribution, it can be notably changed by using different initial distributions, such as the power-law form [23]. This is due to the fact that the flow of energy scale is determined by J_z, which is not drastically renormalized.
[40] V. Dantas and E. C. Andrade, Phys. Rev. Lett. **129**, 037204 (2022).